JOURNAL OF CATALYSIS 152, 291–305 (1995)

# The Preparation of High-Surface-Area Pt/$SiO_2$ Catalysts with Well-Defined Pore Size Distributions

Weiqing Zou and Richard D. Gonzalez[1]

*Department of Chemical Engineering, Tulane University, New Orleans, Louisiana 70118*

Received March 21, 1994; revised December 1, 1994

Thermally stable supported metal catalysts can be prepared by matching the metal particle size to the average pore diameter. Preparative variables aimed at achieving this match are presented. In the 3–8 pH range, blank silica gels prepared using tetraethoxysilane (TEOS) were observed to have BET surface areas of 350–800 $m^2/g$ and mesoporous structures with an average pore diameter of between 4 and 25 nm at a constant $H_2O$/TEOS ratio of 10. Silica aerogels have comparable BET surface areas, larger pore diameters, and pore volumes than xerogels. In the case of supported Pt catalysts prepared by sol–gel synthesis, the effect of preparative variables, including metal precursor, metal loading, reactant stoichiometries, and solvent removal, have been studied. The use of $Pt(AcAc)_2$ resulted in average pore diameters which could be varied in the 4–20-nm range by adjusting the $H_2O$/TEOS ratio during synthesis. BET surface areas in the 500–800 $m^2/g$ and metal dispersions of 50–85% can be achieved. The $H_2$/*n*-hexane reaction was studied on these catalysts. Catalytic activities were found to be comparable or slightly superior to supported metal catalysts prepared by traditional methods.

## INTRODUCTION

In a previous study (1), we have shown that when metal particle sizes are matched to the average pore diameter, the resulting supported metal catalysts show a marked resistance to sintering. In particular, exposure of a Pt/$SiO_2$ xerogel catalyst to flowing oxygen at 675°C for 72 h resulted in negligible sintering. Catalysts prepared by more traditional methods such as impregnation or ion exchange undergo rapid sintering under identical conditions. In these studies, the metal loading was found to be an important variable. Metal loadings below 0.3 wt% resulted in catalysts which were stable in flowing $O_2$ at temperatures below 700°C. At higher temperatures, sintering by vapor-phase transport of the oxide becomes important. When the metal loading exceeded 0.3 wt%, considerable sintering was observed. This resistance to sintering was predicted by Ruckenstein and Pulvermacker (2, 3) using theoretical models. These authors predicted that if the size of a metal crystallite could be matched to the pore diameter, surface diffusion is inhibited and crystal growth will not occur. At metal loadings in excess of 0.3 wt% metal particles may also be present outside of the pore system. These particles readily sinter when exposed to high temperatures in an oxygen atmosphere.

These observations suggest that the preparation of supported metal catalysts in which metal particle diameters are matched to pore diameters may lead to catalysts which have improved thermal properties. To this end we report on variables which enable the control of pore size distributions using the sol–gel synthesis method. The potential advantages of sol–gel processing include purity, homogeneity, and controlled porosity combined with the ability to form large surface area materials at low temperatures. Since metastable, porous structures created in solution are preserved, this leads to applications in filtration, insulation, separations, sensors, and antireflective surfaces (4). An excellent book covering the physics and chemistry of sol–gel processing has been edited by Brinker and Scherer (5). The use of high-surface-area aerogels for catalysts and catalyst supports has been described in a review written by Pajonk (6). In particular, organic derivatives, such as alkoxides, acetates, and acetylacetonates, were used by Teichner *et al.* (7, 8) to prepare a variety of aerogels of $SiO_2$, $Al_2O_3$, $TiO_2$, $ZrO_2$, MgO, and mixed oxides. Unlike the traditional ion exchange and impregnation methods, the metal precursor is added prior to the gelation stage. Using this approach, the metals are incorporated directly into the support framework structure. The method enables a greater degree of control in matching particle sizes to pore diameters. We also report on the catalytic activity and selectivity of these materials in the *n*-hexane/$H_2$ reaction.

---

[1] To whom correspondence should be addressed.

0021-9517/95 $6.00

## EXPERIMENTAL

### *Catalyst Preparation*

*Silica substrate.* Tetraethoxysilane (TEOS) (Johnson Matthey, Ward Hill, MA) was used as the oxide precursor. The procedure followed in sol–gel processing is straightforward. Typically, 10 ml of ethanol together with a variable quantity of water is heated to 50°C in a rotavapor. The pH is adjusted to the designed initial value using either dilute HCl or $NH_4OH$. The TEOS is then added in a dropwise fashion over a period of approximately 4 h. The solution is stirred continuously at 50°C in the rotavapor until a gel is formed. The resulting gel is dried in an oven at 110°C for 12 h. This procedure leads to the formation of a xerogel. The addition of excess ethanol followed by evacuation under supercritical conditions ($T_c$ = 243°C, $P_c$ = 63 atm) in an autoclave results in the formation of an aerogel.

*Supported Pt catalysts.* The compounds used as metal precursors were $Pt(C_5H_7O_2)_2$ [$Pt(AcAc)_2$, Johnson Matthey, Ward Hill, MA], $Pt(NH_3)_4(NO_3)_2$ and $H_2PtCl_6 \cdot xH_2O$ ($x$ = 3–6, Strem Chemicals, Newburyport, MA). A solution consisting of 15 ml tetraethoxysilane (TEOS) and 10 ml ethanol was heated to 45°C and added to a solution containing the designed loading of the metal precursor dissolved in 15 ml of warm acetone (45°C). The resulting solution was stirred continuously for a period of approximately 15 min at 45°C before adding the designed quantity of water. The solution was stirred continuously at 50°C in a rotavapor until a gel was formed. The resulting gel was dried either in a vacuum desiccator ($10^{-3}$ Torr, 1 Torr = 133 N/m$^2$), or in an oven at 110°C for 12 h. Drying was also performed in an autoclave with an excess amount of ethanol under supercritical conditions. The actual metal loading of $Pt/SiO_2$ was measured using inductively coupled plasma (ICP). It is important to point out that in the case of samples prepared by the sol–gel method, the actual metal loading is about 15% less than the designed metal loading. When the TEOS is not completely converted into silica gel, actual metal loadings may exceed designed metal loadings. For this reason, accurate ICP measurements are essential.

For comparison purposes, ion exchange and impregnation preparative methods were also used. $Pt(NH_3)_4(NO_3)_2$ was exchanged onto the surface of a $SiO_2$ aerogel prepared by the sol–gel method. The preparation of the ion-exchanged catalyst is described in detail in Ref. (9). Both $Pt(NH_3)_4(NO_3)_2$ and $Pt(AcAc)_2$ were impregnated on aerogel $SiO_2$ prepared by the sol–gel method. The procedure can be described as follows: aerogel $SiO_2$ is suspended in 25 ml of ethanol and added to a suspension which contains the designed metal loading of the precursor dissolved in 10 ml of warm acetone (45°C). The resulting solution is stirred continuously at 50–80°C until the evaporation of the solvent is complete. The resulting catalyst is dried in an oven at 110°C for 12 h.

*Pretreatment and chemisorption.* Following drying and prior to BET and chemisorption measurements, the samples were pretreated in $O_2$ at 400°C or 1 h followed by reduction in $H_2$ at 400°C for 3 h. $H_2$ and CO chemisorption was performed on a 150–250 mg sample placed in a pyrex microreactor. The gas grade and purification was the same as in Ref. (9). The heating rate of 10°C/min was controlled using a temperature programmer. Tylan mass flow controllers were used to control the flow rate of all gases at 30 ml/min. UHP He or Ar was used to cool the microreactor which contained the sample. Chemisorption measurements were performed using the dynamic pulse method as described by Gonzalez and Sarkany (10). Actual metal loadings (ICP) were used to compute metal dispersions.

*Surface area and pore size distribution.* A 100 or 120 mg sample was placed in a Pyrex holder, preheated to 200°C and outgassed to a final vacuum of $10^{-5}$ Torr. The full sorption (adsorption and desorption) was performed using UHP nitrogen at the normal boiling point of liquid nitrogen (−195.8°C). Surface areas were computed using either the BET or the Langmuir equations as determined by the type of adsorption isotherm. Pore size distributions were obtained using nitrogen desorption.

*Zeta potential of the substrate.* A Doppler electrophoretic light scattering analyzer (Coulter Delsa 440) was used for this study. A dilute and uniform solution of silica was placed in an ultrasonic cleaner and sonicated for a period of 1 min prior to making measurements. The pH values were checked before and after the measurements.

*Electron microscopy.* A Philips EM 410 transmission electron microscope equipped with a $LaB_6$ crystal filament was used for this study. A maximum magnification of ×500,000 and a maximum accelerating voltage of 100 KeV is possible. The specimen preparation and particle analysis are described in Ref. (9).

*$H_2$/n-hexane reaction.* A 99.5% assay of *n*-hexane (Fluka Chemie, Switzerland) and $H_2$ (UHP grade, 99.999%) were used as reactants. Response factors and retention times were calibrated before and following reaction using the standard gases at ppm levels (~15 ppm, Scott Specialty Gases, Houston). Gas-phase *n*-hexane was introduced by bubbling $H_2$ through a saturator maintained at a temperature of 0°C using an ice bath. A flow rate consisting of 1.12 ml/min (at STP: 0°C, 1 atm) was maintained. The $H_2$/*n*-hexane molar ratio was approximately 17. The total flow rate (20 ml/min) was controlled using Tylan mass flow controller. Helium was used as the carrier gas. Gas chromatographic settings were as fol-

lows: oven, $T = 30°C$, injection, $T = 67°C$, and FID detector, $T = 200°C$.

Approximately 150–200 mg of sample were placed in a pyrex microreactor and reduced in flowing $H_2$ at 400°C for 1 h. The final reaction temperature was attained using a heating schedule of 10°C/min controlled by a temperature programmer. A series of data points were obtained at low *n*-hexane conversions (<5%) in order to maintain differential reactor conditions. Catalyst deactivation studies at 400°C were also performed for periods of time ranging from 6–8 h. Catalyst regeneration was performed at 425°C in flowing $O_2$ (UHP grade). Regeneration times were from 4–16 h.

A total of 13 reaction products were separated in the gas chromatographic analysis. For analysis and discussion purposes, these reactions were grouped as follows: hydrogenolysis, isomerization, and cyclization.

## RESULTS

### *Surface Area and Pore Size Distribution of Silica*

Surface areas and average pore size distribution of the resulting xerogels as a function of pH are shown in Fig. 1a. In this study, the molar ratio $H_2O$/TEOS was kept constant at 10 and the gelation temperature was 50°C. A substantial decrease in the surface area together with a concomitant increase in pore size was observed with increasing pH. A sharp decline in surface area was observed at a pH in excess of 8.5. It is also important to note that the pore volume corresponding to meso (2–50 nm) and macro (>50 nm) pores increased at the expense of the micropore (<2.0 nm) volume with increasing pH (Fig. 1b). These pore size classifications are those adapted by IUPAC (11). In general, pore volumes associated with meso- and macropores are about one order of magnitude larger than micropore volumes. The effect of the $H_2O$/TEOS ratio on the surface area at a constant pH of 1.3 is shown in Fig. 2. In this study the gelation temperature was maintained constant at 50°C. A substantial increase in both surface area and the time required for gel formation to occur was observed when the $H_2O$/TEOS ratio was increased from 2 to about 20. It is also important to note that for a $H_2O$/TEOS ratio of 10 and a pH of 1.3, the resulting xerogels had a microporous structure. From the data at 35, 50, and 65°C, the gelation time at pH 1.3 and $H_2O/TEOS = 10$ decreased from 65 to 18 min and the surface area decreased from 990 to 740 $m^2/g$.

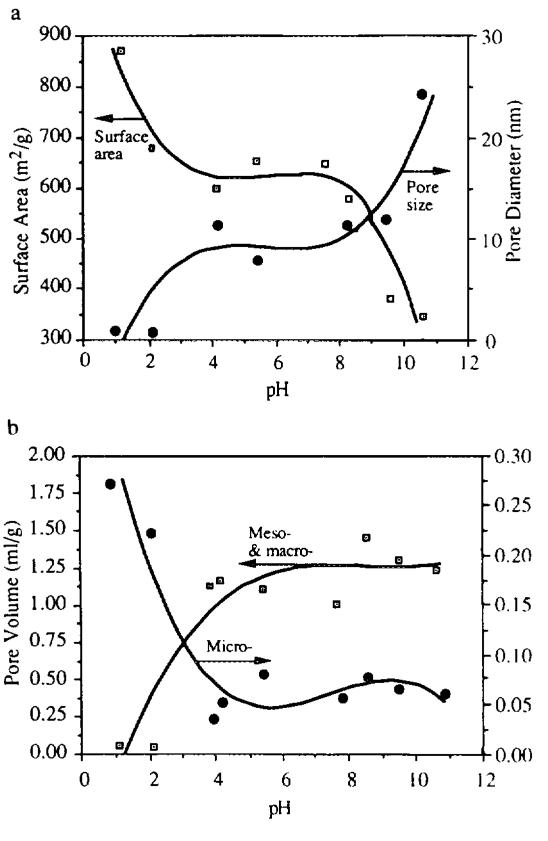

FIG. 1. Changes in: (a) surface area and pore size; (b) micro-, meso-, and macropore volume; as a function of pH at a constant $H_2O$/TEOS ratio of 10, and a gelation temperature of 50°C.

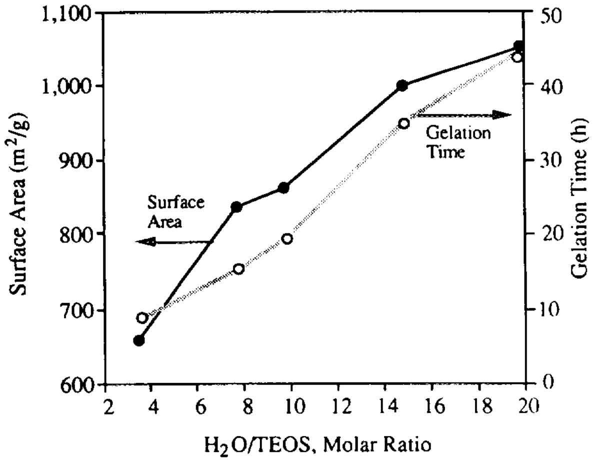

FIG. 2. Changes in surface area and gelation time as a function of the $H_2O$/TEOS ratio at a constant pH of 1.3 and a gelation temperature of 50°C.

Aerogels as catalysts or as catalyst supports have been used for a number of reactions due to their high resistance to heat treatment and their superior mechanical properties. The differences in surface properties of xerogels and aerogels are compared in Table 1. The preparation of these two materials differs only in the procedure used to evaporate the solvent. At a preparation pH of 1.3 and a $H_2O$/TEOS ratio of 15, the xerogel was observed to be microporous and the pressure dependence of the volume of $N_2$ adsorbed was conformed to a Langmuir plot (Type 1). The aerogel, on the other hand, was mesopor-

TABLE 1

A Comparison between Xerogel and Aerogel Silica Supports Prepared at a Constant pH of 1.3, a $H_2O$/TEOS Ratio of 15, and a Gelation Temperature of 50°C

| Sample | Surface area ($m^2/g$) | Pore diameter (nm) | Pore Volume (ml/g) |
|---|---|---|---|
| Xerogel | 1003 | <2 | 0.43 |
| Aerogel | 992 | 18 | 4.36 |

ous and conformed to a BET Type II isotherm (Fig. 3). The pore volume for the aerogel was observed to be approximately one order of magnitude greater than that observed for the xerogel. The thermal stability of xerogels prepared at a pH of 9.0 and a $H_2O$/TEOS ratio of 20 is shown in Table 2. The resulting xerogels were remarkably stable. Heat treatment in air at 600°C for 24 h resulted in a very small loss in surface area and pore volume.

Zeta-potential measurements for a typical xerogel prepared at a pH of 1.23, a $H_2O$/TEOS ratio of 2.6, and a surface area of 259 $m^2/g$ are shown in Fig. 4. The isoelectric point is observed at a pH of 2.0 and is consistent with the isoelectric point obtained for Cab-O-Sil (12) and other silicas (13).

### *Pt/SiO₂ Catalysts Prepared by the Sol–Gel Method*

*Effect of metal precursors.* Three different metal precursors were used in order to form a comparison base for the preparation of $Pt/SiO_2$ catalysts by the sol–gel method. These catalysts were prepared using identical designed metal loadings. The actual metal loadings obtained by ICP were similar for all three catalysts. The microstructure and metal dispersion of the resulting catalysts are summarized in Table 3. When $H_2PtCl_6 \cdot xH_2O$ was used at a $H_2O$/TEOS of 6, the resulting acidic solution (pH ~1.4) resulted in a microporous catalyst which had a rather high surface area (653 $m^2/g$) and a small pore volume (0.28 ml/g). A substantial number of large Pt crystallites were observed using transmission electron microscopy (TEM). These results are shown in Fig. 5a. Good agreement between dispersion measurements performed using hydrogen chemisorption and TEM were obtained (Table 3). When $Pt(NH_3)_4(NO_3)_2$ was used as the metal precursor at a $H_2O$/TEOS ratio 6, the pH of the resulting solution was 4.0. The resulting BET surface area was 480 $m^2/g$ and the average pore diameter was 4 nm. This places it in the mesoporous region. The metal dispersion as measured by both $H_2$ chemisorption and TEM (Fig. 5b) was about 80%. The sample prepared using $Pt(AcAc)_2$ at a $H_2O$/TEOS ratio of 10 resulted in a relatively high-surface-area catalyst. Metal dispersion as measured by both TEM and $H_2$ chemisorption was reasonably high (50%) and the pore volume was much larger than that obtained using $Pt(NH_3)_4(NO_3)_2$. However, several large crystallites were observed by TEM (Fig. 5c).

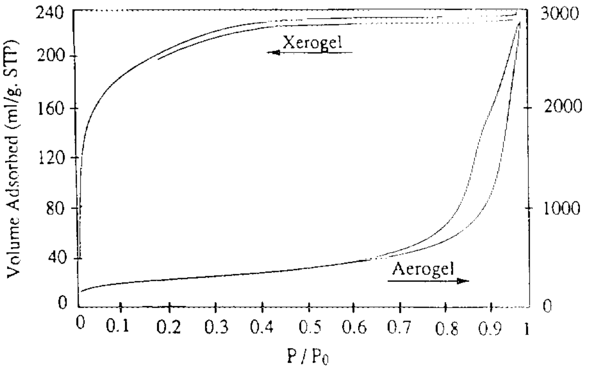

FIG. 3. Different isotherms of the xerogel and the aerogel prepared at a constant pH of 1.3, a $H_2O$/TEOS ratio of 15, and a gelation temperature of 50°C.

*Effect of metal loading.* The effect of metal loading on the physical properties of the $Pt/SiO_2$ catalysts prepared using $Pt(AcAc)_2$ as the metal precursor are summarized in Table 4. In this study, the $H_2O$/TEOS ratio was kept at 10, the pH was ~4.5 and pretreatment was performed in $O_2$ at 400°C for 1 h followed by reduction in $H_2$ at 400°C for 3 h. Actual metal loading as determined by ICP was observed to be about 85% of the designed metal

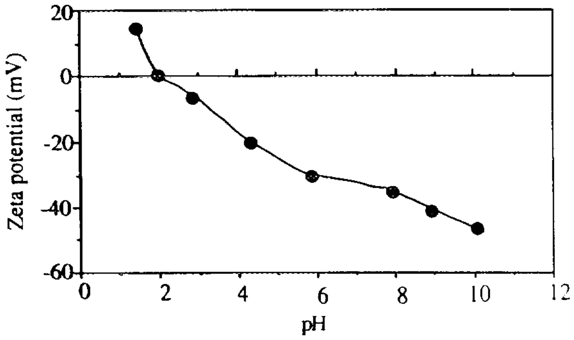

FIG. 4. Changes in the zeta potential as a function of pH for the blank silica prepared by the sol–gel method.

TABLE 2

**Thermostability of Silica Xerogels Prepared at a Constant pH of 9.0, a $H_2O$/TEOS Ratio of 20, and a Gelation Temperature Corresponding to 50°C**

| Heat treatment | Surface area (m$^2$/g) | Pore diameter (nm) | Pore volume (ml/g) |
|---|---|---|---|
| 120°C 24 h in air | 431 | 8 | 0.84 |
| 600°C 24 h in air | 407 | 8 | 0.81 |

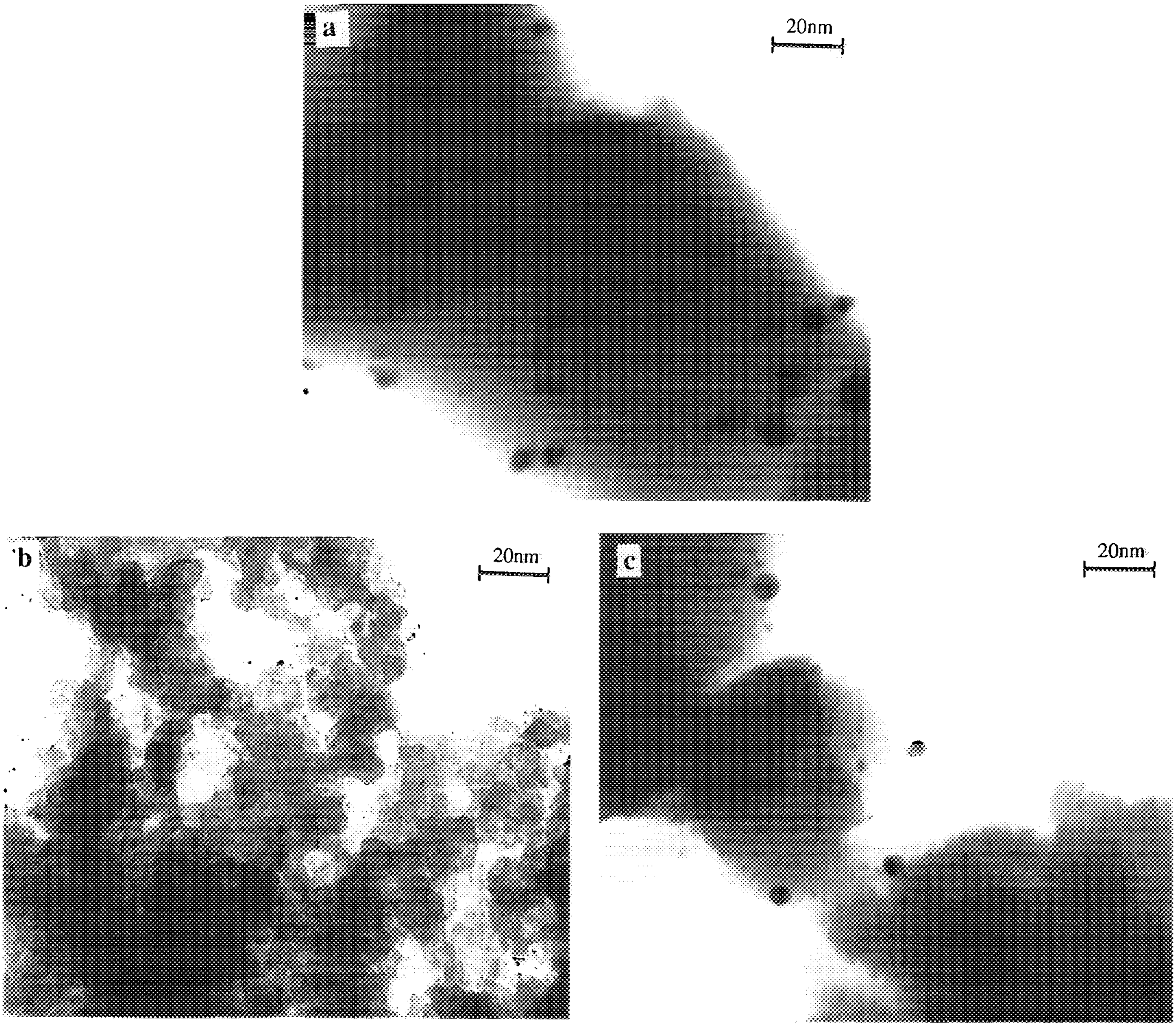

FIG. 5. Transmission electron micrographs of resulting gels under the same pretreatment conditions: $O_2$ at 400°C for 1 h, $H_2$ at 400°C for 3 h: (a) $[PtCl_6]^{2-}/SiO_2$; (b) $[Pt(NH_3)_4]^{2+}/SiO_2$; (c) $Pt(AcAc)_2/SiO_2$.

### TABLE 3

**The Effect of Different Metal Precursors on the Surface Properties of Supported Xerogels: Designed Metal Loading of 2 wt%, Pretreatment in $O_2$ at 400°C for 1 h, and $H_2$ at 400°C for 3 h**

| Metal precursor | ICP (wt%) | $H_2O$/TEOS | pH | BET ($m^2/g$) | Pore diameter (nm) | Pore volume (ml/g) | Dispersion | |
|---|---|---|---|---|---|---|---|---|
| | | | | | | | $D_H$ | TEM |
| $H_2PtCl_6 \cdot 6H_2O$ | 1.76 | 6 | 1.4 | 653 | <2 | 0.28 | 18 | 20 |
| $Pt(NH_3)_4(NO_3)_2$ | 1.62 | 6 | 4.0 | 480 | 4 | 0.31 | 74 | 80 |
| $Pt(C_5H_7O_2)_2$ | 1.65 | 10 | 4.8 | 632 | 16 | 1.29 | 48 | 50 |

### TABLE 4

**The Effect of Metal Loading on the Properties of $Pt/SiO_2$ Xerogels Prepared Using $Pt(AcAc)_2$ as the Metal Precursor: pH ~5, a $H_2O$/TEOS Ratio of 10, Pretreatment in $O_2$ at 400°C for 1 h, and $H_2$ at 400°C for 3 h**

| Designed loading (wt%) | ICP (wt%) | BET ($m^2/g$) | Pore diameter (nm) | Pore volume (ml/g) | Metal dispersion (%) | | |
|---|---|---|---|---|---|---|---|
| | | | | | $D_{CO}$ | $D_H$ | TEM |
| 2.0 | 1.65 | 632 | 16 | 1.29 | 46 | 48 | 50 |
| 1.0 | 0.80 | 706 | 8 | 0.86 | 70 | 75 | 80 |
| 0.75 | 0.65 | 759 | 7 | 0.84 | 70 | | 80 |
| 0.5 | 0.40 | 586 | 12 | 1.09 | 85 | 80 | 80 |

### TABLE 5

**The Effect of the $H_2O$/TEOS Ratio on the Physical Properties of $Pt/SiO_2$ Xerogels: pH ~4.8, Designed Metal Loading 2 wt%, Pretreatment in $O_2$ at 400°C for 1 h, and $H_2$ at 400°C for 3 h**

| $H_2O$/TEOS | ICP (wt%) | BET ($m^2/g$) | Pore diameter (nm) | Pore volume (ml/g) | Metal dispersion (%) | | |
|---|---|---|---|---|---|---|---|
| | | | | | $D_{CO}$ | $D_H$ | TEM |
| 3 | 5.8 | 474 | 20 | 1.78 | 8 | | |
| 6 | 2.8 | 495 | 15 | 1.34 | 18 | 21 | 20 |
| 10 | 1.65 | 632 | 16 | 1.29 | 46 | 48 | 50 |
| 15 | 1.65 | 721 | 8 | 0.96 | 40 | 49 | |
| 20 | 1.65 | 784 | 4 | 0.62 | 45 | 50 | |

### TABLE 6

**The Effect of Solvent Removal on the Surface Properties of Xerogels and Aerogels Using $Pt(AcAc)_2$ as the Metal Precursor: a $H_2O$/TEOS Ratio of 10, pH 4.3, Designed Metal Loading of 1.0 wt%, Pretreatment in $O_2$ at 400°C for 1 h, and $H_2$ at 400°C for 3 h**

| Sample | ICP (wt%) | BET (m2/g) | Pore diameter (nm) | Pore volume (ml/g) | Metal dispersion (%) | | |
|---|---|---|---|---|---|---|---|
| | | | | | $D_{CO}$ | $D_H$ | TEM |
| Xerogel | 0.80 | 706 | 7.5 | 0.86 | 70 | 75 | 80 |
| Aerogel | 0.80 | 891 | 40 | 1.84 | 9 | 8 | 5–10 |

loading. A maximum in the BET surface area was observed for a designed metal loading of 0.75 wt% Pt. Average pore diameter and pore volume corresponding to this metal loading were observed to be a minimum. Metal dispersion obtained using either CO or $H_2$ chemisorption was observed to increase from 50 to 85% as the designed metal loading was decreased. Agreement between CO and $H_2$ chemisorption was good. TEM measurements agreed reasonably well with results obtained using chemisorption. A reduction in the designed metal loading below 0.5 wt% did not result in an improvement in the dispersion to above 85%. However, TEM measurements for highly dispersed catalysts are somewhat unreliable due to failure to observe very small particles. Additionally, chemisorption measurements for very low metal loadings are difficult to perform and have a high degree of uncertainty.

*Effect of $H_2O$/TEOS ratio.* The effect of reactant stoichiometries on the physical properties of the Pt/SiO$_2$ xerogel catalysts was studied by varying the $H_2O$/TEOS ratio from 3 to 20. All other preparative variables were kept constant. The designed metal loading was 2 wt%, the pH was ~4.8 and pretreatment was in $O_2$ at 400°C for 1 h followed by reduction in $H_2$ at 400°C for 3 h. The results of this study are summarized in Table 5. $H_2O$/TEOS ratios in excess of 10 resulted in constant metal loadings of 1.65% as determined by ICP. The use of low $H_2O$/TEOS ratios resulted in actual metal loading in excess of the designed metal loading. The BET surface area was observed to increase monotonically with increasing $H_2O$/TEOS ratio at the expense of pore volume and average pore diameter. The average pore size distribution as a function of the $H_2O$/TEOS ratio is shown in Fig. 6. The use of low $H_2O$/TEOS ratios resulted in a broadening of the pore size distribution. A narrow and much sharper pore size distribution was obtained for a $H_2O$/TEOS ratio of 20. The metal dispersion appeared to remain constant following the attainment of 100% TEOS conversion.

*Supported xerogel and aerogel catalysts.* This study was performed starting with a $H_2O$/TEOS ratio of 10 and a designed metal loading corresponding to 1 wt% Pt. The resulting gel was divided into two aliquot portions. The first of these aliquot portions was dried in an oven at 110°C for 12 h. To the second aliquot, 250 ml of ethanol was added followed by solvent removal in an autoclave under supercritical conditions. Both aliquots were pretreated under identical conditions prior to performing characterization studies.

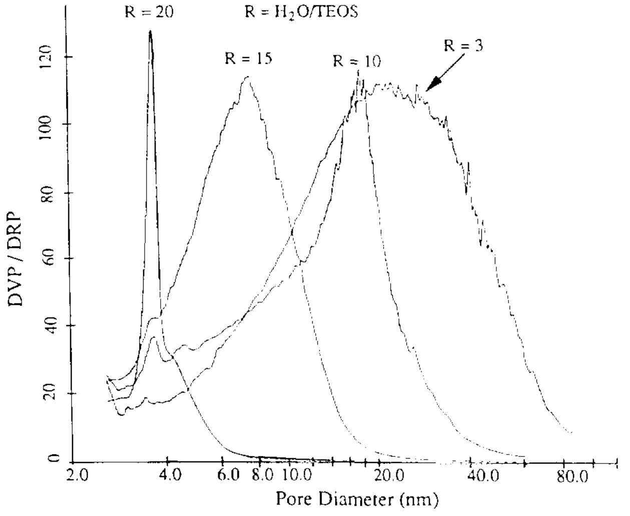

FIG. 6. Changes in pore size distributions as a function of the $H_2O$/TEOS ratio under the same designed metal loading of 2 wt%.

Both the xerogel and the aerogel had ICP metal loadings of 0.80 wt%. BET surface areas were 706 and 891 m$^2$/g, respectively, for the xerogel and the aerogel. Solvent evacuation under supercritical conditions resulted in an increase in the average pore diameter from 7.5 to 40.0 nm for the aerogel catalysts. The pore volume for the aerogel catalysts was also observed to increase from 0.86 to 1.84 ml/g. However, metal dispersions were considerably lower for the aerogel catalysts (5–10%) than those observed for the xerogel catalysts (75%). These observations were confirmed using TEM (Figs. 7a and 7b). A small uniform size distribution was observed for the xerogel catalysts, while large crystallites were found for the aerogel materials. These data are summarized in Table 6.

*Impregnation and ion exchange of Pt metal precursors onto silica prepared by the aerogel method.* Impregnation of $Pt(NH_3)_4(NO_3)_2$ onto the high-surface-area aerogel by the sol–gel method was performed. In this study, the metal precursor was dissolved in acetone and the aerogel support was suspended in ethanol. The BET surface area of the impregnated sample increased from 992 to 1097 m$^2$/g. However, the average pore diameters and pore volumes were observed to decrease significantly (Table 7). The average Pt particle size as measured by both $H_2$ chemisorption and TEM was approximately 6.5 nm. In order to compare the impregnated materials to ion-exchanged catalysts, the pH of the precursor–water solution was increased to a value in excess of its isoelectric point through the addition of dilute $NH_4OH$. $Pt(NH_3)_4(NO_3)_2$ was exchanged onto the aerogel–water solution at a pH of ~8.0. The resulting supported catalysts showed a substantial loss in both BET surface area and pore volume. Pt crystallite sizes were observed to be 3.5 nm by TEM. In addition to this observation, a bimodal pore size distribution was obtained (Fig. 8). The average pore size distribution of unsupported silica aerogel is also shown in Fig. 10 for comparison purposes.

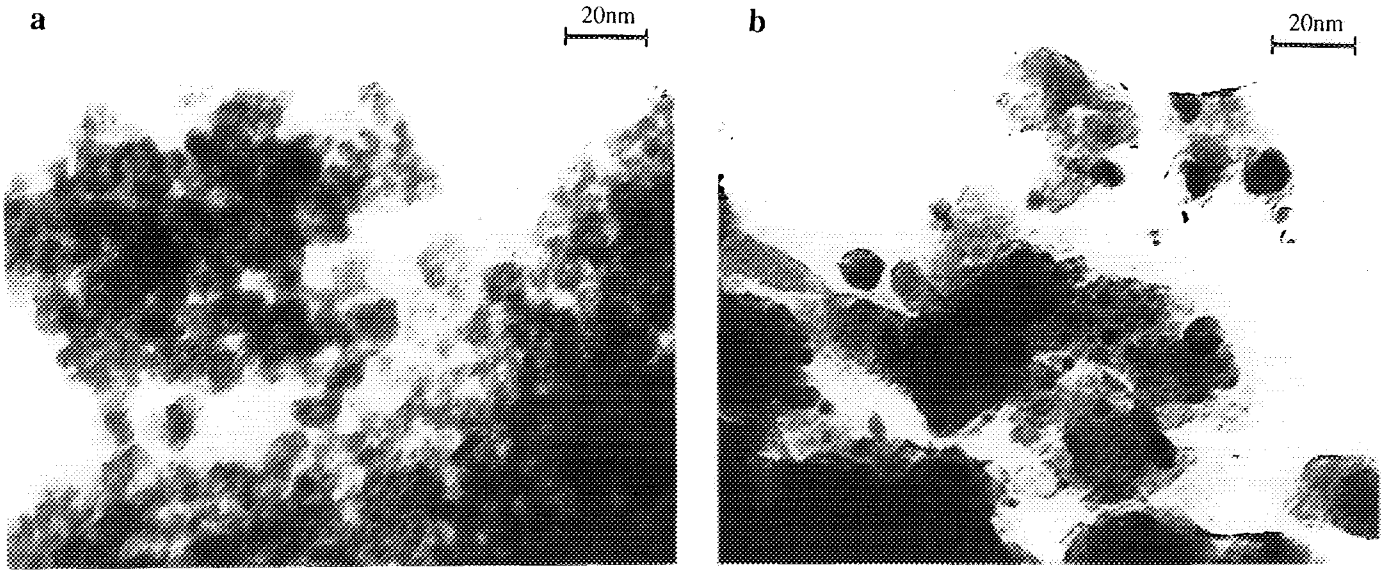

FIG. 7. Transmission electron micrographs of $Pt(AcAc)_2/SiO_2$ prepared using a $H_2O$/TEOS ratio of 10, a designed metal loading of 1 wt% and following pretreatment in $O_2$ at 400°C for 1 h, $H_2$ at 400°C for 3 h: (a) xerogel catalyst; and (b) aerogel catalyst.

The use of $Pt(AcAc)_2$ as a metal precursor in place of $Pt(NH_3)_4(NO_3)_2$ onto the silica aerogel was attempted using impregnation. The microstructure of the resulting catalyst was similar to that of the unsupported aerogel material. TEM data showed an average particle size of 6 nm. $H_2$ chemisorption resulted in a Pt dispersion of 13% on the support (Table 8).

### *$H_2$/n-Hexane Reactions*

The physical properties of four $Pt/SiO_2$ catalysts used as a comparison basis set to study the $H_2$/*n*-hexane reaction are summarized in Table 9. In all cases the use of a designed metal loading of 1 wt% resulted in comparable ICP metal loadings of between 0.65 and 0.91 wt%. $Pt/SiO_2$ catalysts prepared using either xerogels or aerogels had BET surface areas of approximately 800 $m^2/g$. The $Pt/SiO_2$ catalyst prepared by ion-exchanging $Pt(NH_3)_4(NO_3)_2$ onto Cab-O-Sil had a much lower BET surface area (~200 $m^2/g$). The $Pt/SiO_2$ xerogel had smaller pore diameters and pore volumes than the other catalysts. Another set of $Pt/SiO_2$ catalysts from Northwestern University prepared by ion-exchanging $Pt(NH_3)_4Cl_2$ onto silica gel (Davison Grade 62) were used. The silica support had a BET surface area of 295 $m^2/g$, a pore diameter of 14 nm, and a pore volume of 1.20 ml/g. The catalyst had a metal loading of 0.83 wt% and a metal dispersion of 75%. Detailed preparation and characterization are described in Ref. (14). Very high metal dispersions were obtained for the xerogel (75%) and the ion-exchanged $Pt/SiO_2$ (80%). The impregnation of aerogel samples resulted in much lower dispersions (15%). The $Pt/SiO_2$ aerogel catalyst resulted in very poor Pt metal dispersions (10%).

Reactions attributed to thermal cracking in the 250–425°C temperature range were tested using blank silica.

TABLE 7

The Effect of the Adsorption of $Pt(NH_3)_4(NO_3)_2$ on the Surface Properties of Supported Aerogels under Constant Pretreatment Conditions: $O_2$ at 400°C for 1 h and $H_2$ at 400°C for 3 h

| Method | pH | Designed loading (wt%) | ICP (wt%) | BET ($m^2/g$) | Pore diameter (nm) | Pore volume (ml/g) | Dispersion (%) $D_H$ | Dispersion (%) TEM |
|---|---|---|---|---|---|---|---|---|
| $SiO_2$ Aerogel | 1.4 | | | 992 | 20 | 4.36 | | |
| Impregnation | 2.4 | 1.0 | 0.91 | 1097 | 8 | 1.67 | 10 | 15 |
| Ion exchange | 8.0 | 2.0 | 0.95 | 714 | 4, 7 | 0.94 | 25 | 28 |

TABLE 8

**The Effect of the Adsorption of Pt(AcAc)$_2$ on the Surface Properties of Supported Aerogels under the Same Pretreatment Conditions: O$_2$ at 400°C for 1 h and H$_2$ at 400°C for 3 h**

| Method | pH | Designed loading (wt%) | ICP (wt%) | BET (m$^2$/g) | Pore diameter (nm) | Pore volume (ml/g) | Dispersion (%) | |
|---|---|---|---|---|---|---|---|---|
| | | | | | | | $D_H$ | TEM |
| SiO$_2$ Aerogel | 1.40 | | | 783 | 11 | 2.63 | | |
| Impregnation | 1.65 | 1.0 | 0.91 | 754 | 11 | 2.62 | 10 | 13 |

The particular silica used for this background study was a xerogel silica prepared using a H$_2$O/TEOS ratio of 10, a pH of 4.2, and a gelation temperature of 50°C. It had a BET surface area of 600 m$^2$/g, an average pore diameter of 12 nm, and a pore volume of 1.17 ml/g. Conversion of *n*-hexane over this blank silica was not observed in this temperature range.

The catalytic activity as measured by the *n*-hexane conversion and TOF at the same reaction temperature of 400°C is summarized in Table 9. The Pt/SiO$_2$ xerogel showed the highest conversion of *n*-hexane (42.6%) and TOF ($65 + 10^{-3}$ molec./site s) among the five catalysts studied. Two ion-exchanged Pt/SiO$_2$ catalysts, Pt(NH$_3$)$_4$(NO$_3$)$_2$/Cab-O-Sil, and Pt(NH$_3$)$_4$Cl$_2$/Davison, showed similar reaction activities. The TOF as measured by the number of *n*-hexane molecules converted per site per second was approximately constant for the four other catalysts studied (i.e., $35–53 \times 10^{-3}$ molec./site s). In this study, sample weights were approximately 200 mg, *n*-hexane flow rate to the reactor was 1.12 ml/min, and the H$_2$/*n*-hexane ratio was kept constant at 17. From these data it appears that the catalytic activity as measured by the TOF is not strongly dependent on dispersion or method of preparation.

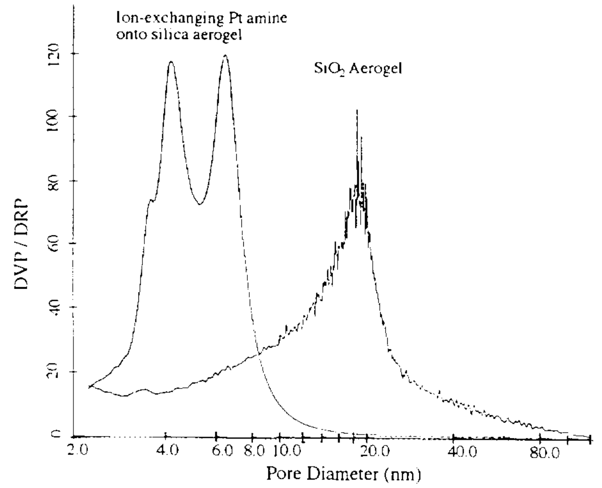

FIG. 8. Changes in pore size distribution as a result of ion-exchanging Pt(NH$_3$)$_4$(NO$_3$)$_2$ onto the surface of aerogels.

A study was performed in order to compare the resistance to deactivation for the four different catalysts studied. This study was performed at 400°C under reaction conditions similar to those used in the catalytic activity study. First order deactivation rate constants were calculated using the method outlined by Levenspiel (15) on the assumption that plug flow was maintained. These data are summarized in Table 10. First order deactivation rate constants for both the xerogel and the ion-exchanged catalysts are comparable and are lower than those calculated for the impregnated and the aerogel catalysts. These results are in agreement with similar studies in the literature which suggest that coke formation is favored on large metal ensembles and is therefore a surface-sensitive reaction. The activation energies for the formation of $C_1$ and $C_2$ products have been included in Table 10. The activation energy ratio $C_2/C_1$ was approximately 0.5 for both the xerogel and the ion-exchanged Pt/SiO$_2$ catalysts. A ratio of about 1 was observed for both the impregnated and the aerogel catalysts. Linear Arrhenius plots were obtained for the formation of these products in the 280–330°C temperature range. Two Arrhenius plots of the xerogel and the impregnated Pt/SiO$_2$ catalysts are shown in Fig. 9.

Changes in the physical properties of the catalysts following deactivation are summarized in Table 9 for comparison purposes. Some loss in metal dispersion, BET surface area, and pore volume was observed for all five catalysts. The decrease in surface area and pore volume observed for the ion-exchanged catalysts was somewhat lower. However, the loss in catalytic activity as measured by the change in the TOF was about the same ($14–20 \times 10^{-3}$ molec./site s) for the five catalysts studied. Partial regeneration occurred following treatment in an O$_2$ flow for 16 h at 425°C. A 2-h treatment in flowing O$_2$ at the same temperature had no effect. The catalyst regeneration study is summarized in Table 11.

Selectivities for hydrogenolysis, isomerization, and cyclization reactions are shown in Fig. 10. The selectivities corresponding to hydrogenolysis of the xerogel and the

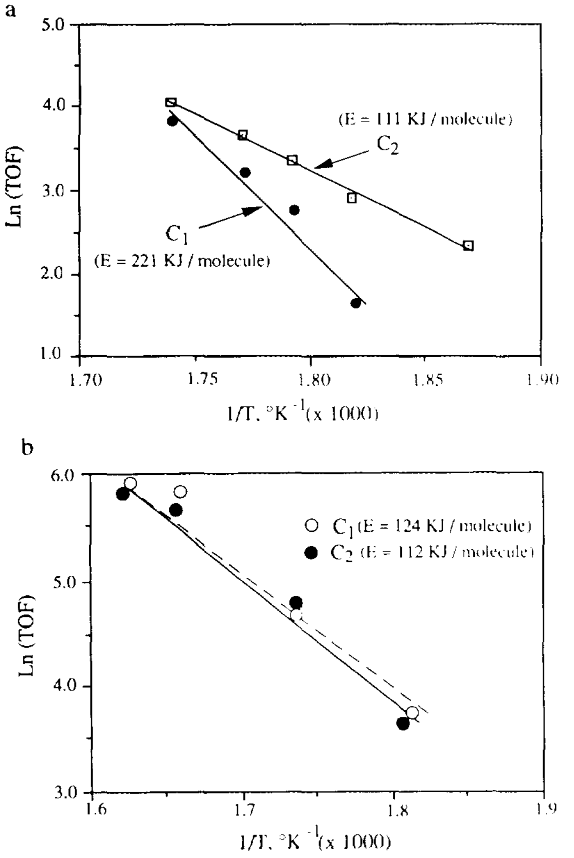

FIG. 9. Arrhenius plots for $C_1$ and $C_2$ as a function of temperature: (a) xerogel catalyst; and (b) impregnated catalyst.

ion-exchanged catalyst were nearly identical over the entire *n*-hexane conversion range studied. The Pt/SiO$_2$ aerogel catalyst and the catalyst prepared by impregnation were very selective for hydrogenolysis at low *n*-hexane conversion (Fig. 10a). We believe that the large drop in selectivity obtained over the large particles is due to a greater activity for carbon formation. At conversions in excess of 2%, hydrogenolysis takes place over carbon-covered sites. The selectivity for isomerization and cyclization reactions as a function of conversion were similar for the ion-exchanged catalysts (Fig. 10b). The aerogel catalyst showed an unusually high selectivity for cyclization reactions at low conversion (Fig. 10c). From these data it is apparent that hydrogenolysis occurs preferentially on large particles while isomerization occurs primarily on small particles. Cyclization appears to be less sensitive to particle size effects. However, the selectivity to cyclized products appears to occur to a greater extent over the xerogel and the ion-exchanged catalysts and is not observed to decrease dramatically at low conversions.

## DISCUSSION

### *Blank Xerogel and Aerogel Silica*

In the sol–gel process, the starting materials are metal alkoxides which have organic ligands attached to central silicon or aluminum atoms. Silica gels are most often synthesized by hydrolyzing monomeric precursors using mineral acids (i.e., HCl) or bases (i.e., NH$_4$OH) as catalysts (5). At a functional group level these reactions have received considerable attention in the literature (5). The relative rates of hydrolysis and condensation reactions as a function of pH have been reported by Keefer (16). When the pH is below 2, the rate of hydrolysis is large compared to the rate of condensation. When the H$_2$O/TEOS ratio is greater than 4, hydrolysis will be essen-

TABLE 9

Changes in the Physicochemical Properties of Pt/SiO$_2$ Catalysts before and after Deactivation under Reaction Conditions: 400°C, H$_2$/*n*-Hexane Molar Ratio of 17

| Catalyst | ICP (wt%) | BET (m$^2$/g) | Pore diameter (nm) | Pore volume (ml/g) | Chemisorption $D_H$ (%) | *n*-Hexane Conv. (%) | TOF × 10$^3$ (molec./site s) |
|---|---|---|---|---|---|---|---|
| Xerogel[a] | 0.80 | 729 | 7.0 | 0.78 | 75 | 42.60 | 65 |
| Xerogel[b] | | 690 | 7.0 | 0.72 | 68 | 26.83 | 45 |
| Ion exchange[a] | 0.65 | 205 | 24 | 1.38 | 80 | 28.76 | 48 |
| Ion exchange[b] | | 193 | 24 | 1.31 | 70 | 15.88 | 30 |
| 81IonXS[a,c] | 0.83 | 295 | 14 | 1.30 | 75 | 45.54 | 53 |
| 81IonXS[b] | | 284 | 14 | 1.27 | 55 | 22.79 | 36 |
| Impregnation[a] | 0.91 | 754 | 11 | 2.62 | 15 | 5.56 | 38 |
| Impregnation[b] | | 786 | 11 | 2.61 | 12 | 3.04 | 24 |
| Aerogel[a] | 0.80 | 891 | 40 | 1.84 | 10 | 3.10 | 35 |
| Aerogel[b] | | 800 | 40 | 2.04 | 9 | 1.38 | 18 |

[a] Fresh catalysts after the standard pretreatment in O$_2$ at 400°C for 1h, H$_2$ at 400°C for 3 h.

[b] Deactivated catalysts after reaction in H$_2$/*n*-hexane at 400°C for 6–8 h.

[c] Samples from J. B. Butt's group in Northwestern University.

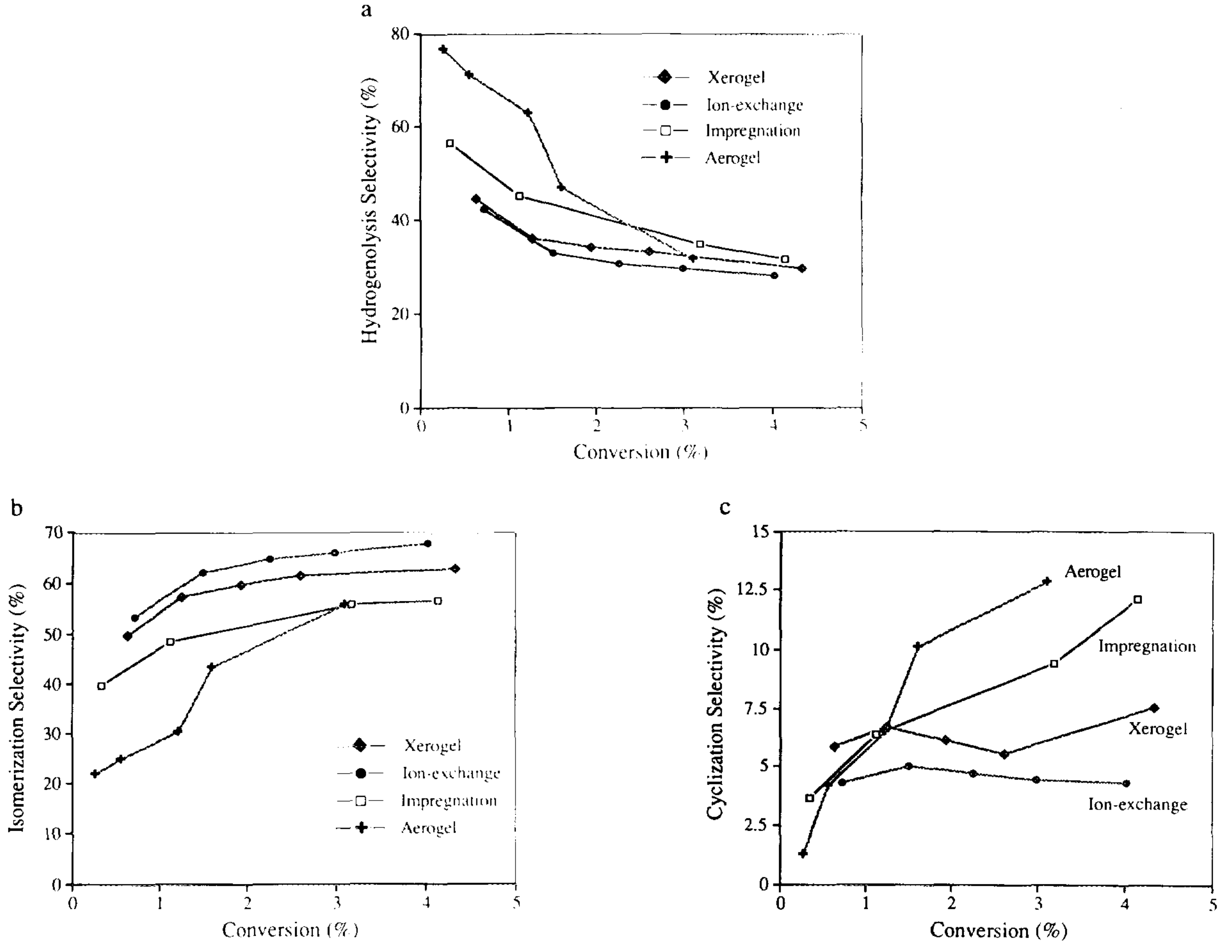

FIG. 10. Specific selectivity as a function of conversion for different Pt/SiO$_2$ catalysts: (a) hydrogenolysis reaction; (b) isomerization reaction; and (c) cyclization reaction.

tially complete at an early stage in the reaction (5). When a pH of 1.3 and a $H_2O$/TEOS ratio of 10 were used, the resulting xerogels had a high surface area (~1000 m$^2$/g) and small average pore diameter (<2 nm). Type I isotherms correspond to the microporous materials due to the adsorption and desorption of gas-phase nitrogen at low $P/P_0$ ratios (0.008–0.01). Intermediate values of the pH (3–8) represent conditions in which a spectrum of transitional structures might be expected. The rate of hydrolysis decreases while the rate of condensation increases with increasing pH. Above a pH of 9, hydrolysis and condensation occur by bimolecular nucleophilic dis-

TABLE 10

First Order Deactivation Rate Constants Based on the Disappearance of *n*-Hexane and Activation Energies of $C_1$ and $C_2$ Formation for Different Pt/SiO$_2$ Catalysts

| Catalysts | Particle size (nm) | Activation energy (KJ/mol, 280–330°C) $C_1$ | $C_2$ | Deactivation rate constant $K_d \times 10^3$ (h$^{-1}$) at 400°C |
|---|---|---|---|---|
| Ion exchange | 1.5 | 187 | 91 | 218 |
| Xerogel | 1.7 | 221 | 111 | 221 |
| Impregnation | 6.0 | 124 | 112 | 265 |
| Aerogel | 10.5 | 121 | 132 | 328 |

TABLE 11

Regeneration of $Pt/SiO_2$ Xerogel Catalysts at Different Conditions

| Catalyst | BET ($m^2/g$) | Pore diameter (nm) | Pore volume (ml/g) | Chemisorption $D_H$ (%) | *n*-Hexane Conv. (%) | TOF × $10^3$ (Molec./site s) |
|---|---|---|---|---|---|---|
| Fresh[a] | 729 | 7.0 | 0.78 | 75 | 42.60 | 65 |
| Deactivated[b] | 690 | 7.0 | 0.72 | 68 | 26.83 | 45 |
| Regenerated[c] | | | | | 25.20 | |
| Regenerated[d] | 713 | 7.0 | 0.74 | 73 | 32.50 | 54 |

[a] Pretreated in $O_2$ at 400°C for 1 h and $H_2$ at 400°C for 3 h.

[b] Reacted in $H_2/n$-hexane at 400°C for 7 h.

[c] Regenerated in $O_2$ at 425°C for 2 h and $H_2$ at 400°C for 2 h.

[d] Regenerated in $O_2$ at 425°C for 16 h and $H_2$ at 400°C for 2 h.

placement reactions involving $OH^-$ and $SiO^-$ anions, respectively. These two reactions are related to the production of monomers. The dominant reaction is the dissolution of Si–O–Si linkages to provide a continuous source of monomers. The resulting gel has a low BET surface area and a large average pore diameter. When the pH was adjusted to 8.5 a BET surface area of 350 $m^2/g$ was obtained. The synthesis in the intermediate pH range (3–8) is characterized by a mesoporous structure with surface areas decreasing from 800 to 350 $m^2/g$. In this pH range, the average pore diameter was observed to increase from 4 to 25 nm for a constant $H_2O/TEOS$ ratio of 10. Type II BET isotherms were observed in this pH range for a $P/P_0$ range of 0.05–0.25.

Because water is produced as a by-product in the condensation reaction, a $H_2O/TEOS$ ratio of 2 should lead to complete hydrolysis and condensation with the formation of an anhydrous silica product as shown by

$$n\,(Si(OR)_4 + 2n\,H_2O \rightarrow n\,SiO_2 + 4n\,ROH. \quad [1]$$

However, even in excess water ($H_2O/TEOS > 2$), the reaction does not go to completion. A spectrum of intermediate species, which conform to the general formula $[SiO_x(OH)_y(OR)_z]_n$, with $2x + y + z = 4$, are generated (5). For this reason, the percentage conversion of silica must be known in order to calculate the final metal loading. The use of ICP to obtain an accurate measure of the Pt loading is, therefore, essential. Aelion *et al.* (17) observed that the acid-catalyzed hydrolysis of TEOS was first order in $[H_2O]$. However, under basic conditions, the reaction was close to zero order in the concentration of $[H_2O]$. In this study, the surface area was observed to increase with increasing $H_2O/TEOS$ ratio under acid-catalyzed conditions (pH 1.3) and a gelation temperature of 50°C. Because the rate of hydrolysis is first order in the concentration of $H_2O$, an increase in the $H_2O/TEOS$ ratio will result in an increase in the rate of hydrolysis. The condensation reaction on the other hand is a net $H_2O$ producer. For this reason, the rate at which condensation occurs is inhibited by an increase in the $H_2O/TEOS$ ratio and the gelation time is also expected to increase as observed. An increase in the concentration of $H_2O$ favors the formation of silica as evidenced by the stoichiometry of the overall reaction.

The solubility of amorphous silica as a function of pH at different temperatures has been investigated by Iler (18). The solubility of silica increases with increasing temperature at constant pH. This increase in solubility results in an increase in particle size and, consequently, a decrease in surface area. This is also consistent with observations obtained in this study.

Capillary forces arise from the difference between solid–vapor and solid–liquid interfacial energies. The huge interfacial area of the gel (~300–1000 $m^2/g$) can result in capillary pressure as large as ~100 MPa(5). Because it is possible to develop large pressure gradients within the gel structure, the network is compressed to a greater extent at the exterior surface. This differential strain results in cracking. Solvent removal under supercritical drying conditions (243°C and 63 atm) results in the elimination of the liquid–vapor interface and a preservation of the gel microstructure. A comparison in the microstructure of the xerogel and the aerogel under identical $H_2O/TEOS$ ratio and a pH of 1.3 is shown in Fig. 3 and Table 1. It is evident that the $N_2$ adsorption behavior is quite different. For the xerogel, the adsorption of $N_2$ is distinctly Langmuir, while $N_2$ adsorption on the aerogel follows a BET Type II adsorption isotherm behavior. Pore volumes for the aerogel and the xerogel differ by an order of magnitude.

Teichner *et al.* (7) studied the thermal stability of aerogels heated in air at increasing temperatures. The conclusions reached by his group are in agreement with those obtained in this study. Heating in air at 600°C resulted in only a minor decrease in surface area (Table 2).

### *Pt/SiO$_2$ Catalysts Prepared by the Sol–Gel Method*

*Effect of metal precursor.* A variety of metal precursors and synthetic techniques have been used to disperse metals onto the surface of xerogels and aerogels. Lopez *et al.* (19) added TEOS in a dropwise fashion to a solution consisting of hexachloroplatinic acid dissolved in a mixture of ethanol. Armor *et al.* (20) added a solution of aluminum *sec*-butoxide to a second solution consisting of palladium acetate dissolved in warm acetone. The designed quantity of water was added during the final stages of preparation in order to complete the hydrolysis. The physicochemical properties of the resulting gels have received considerable attention. However, metal dispersions as a function of the preparative variables have recieved little attention in the literature. In preliminary studies, $RuCl_3$, and $H_2PtCl_6 \cdot xH_2O$ were used as metal precursors. TEOS was added in a dropwise fashion to a mixture consisting of ethanol, water, and the metal precursor. When the synthesis was carried out under acid conditions (pH ~1.4), the metal dispersion averaged between 5–10%. These results lead to the speculation that the metal atoms appear to be occluded as a result of the addition of water during early stages in the reaction (21). In this study, the sol–gel synthesis method used by Armor (20) was used in the preparation of Pt/SiO$_2$. When $H_2PtCl_6 \cdot xH_2O$ was used, the UV spectrum of $[PtCl_6]^{2-}$ in solution was essentially identical to the diffuse UV reflectance spectra of the species adsorbed on the surface (22). This suggested little or no perturbation of the Pt precursor following adsorption and solvent removal to form the xerogel. Because the pH of the $H_2PtCl_6 \cdot xH_2O$ solution was about 1.4, the zeta potential of silica in contact with the precursor was close to that corresponding to the isoelectric point (pH 1.5–2.0, Fig. 4). For this reason, the interaction between the surface and the negatively charged metal precursor is weak or slightly repulsive. Because TEM and hydrogen chemisorption were in agreement, the occlusion of Pt by the support can be ruled out. The low metal dispersion observed is, in all likelihood, due to the weak interaction between the precursor and the support.

When $Pt(NH_3)_4(NO_3)_2$ was used as the metal precursor, a comparison of the UV spectra of the precursor in solution and that of the precursor adsorbed on the solid suggested little or no perturbation of the precursor following adsorption (22). At a pH of 4.0 corresponding to that of the dissolved precursor in acetone, the surface of the silica is negatively charged. The interaction between the positively adsorbed cations and the negatively charged surface is strong. Under these conditions, dispersions are much higher. The disadvantage of using this precursor is one of limited solubility in acetone and rather low BET surface areas and pore volumes.

The low BET surface areas and pore volumes obtained using $Pt(NH_3)_4(NO_3)_2$ prompted us to try an organic metal precursor. $Pt(AcAc)_2$ has a high solubility in acetone at 45°C. The UV spectra of the solution showed that the structure of $Pt(AcAc)_2$ was preserved during the gelation reaction. Because of the organic ligand attachment to Pt, the ionic interaction between the metal precursor and the support is rather weak at a measured pH of 4.8. The observed dispersion of Pt was in between that observed using $H_2PtCl_6 \cdot xH_2O$ (repulsive interaction) and $Pt(NH_3)_4(NO_3)_2$ (attraction interaction). Metal dispersion, BET surface areas and pore volumes using $Pt(AcAc)_2$ were acceptable (Table 3).

Because one of the goals of this study is to match the metal particle size to the average pore diameter, it is evident that none of the catalysts described in Table 3 are satisfactory. Pore diameters are considerably larger than particle sizes. However, an increase in the $H_2O$/TEOS ratio to a value of 60 results in average pore sizes of 3.5 nm (1). For this reason, catalysts with a Pt dispersion corresponding to approximately 40% provide the desired match.

*Effect of metal loading.* In the sol–gel synthesis the pH of the final solution used prior to the addition of water was approximately 4.5. This solution contained acetone, ethanol, the metal precursor, and TEOS. Nothing else was added in order to adjust the pH. The negative charge at the silica surface is about one half of that measured at a pH of 9. In addition to this lower negative charge at the surface, the organometallic precursor $Pt(AcAc)_2$ inhibits Pt atom polarity due to its organic ligands. The precursor–surface interaction is therefore weak, and for this reason, the Pt metal dispersion will depend to a much larger extent on the overall metal loading. Additionally, the resulting silica gel is not washed to remove weakly chemisorbed species. The use of a $H_2O$/TEOS ratio of 10 and a pH of 4.2, resulted in a BET surface area of 600 m$^2$/g and an average pore diameter of 12 nm. This result is not that different to that obtained for Pt xerogel catalysts. However, we should qualify these remarks by noting that the BET surface area appears to be a maximum and the pore volume a minimum for a designed metal loading corresponding to 0.75 wt%. It is important to note that metal dispersions of 85% can be obtained at very low Pt metal loadings.

*Effect of the $H_2O$/TEOS ratio.* The ability to change pore size distributions by carefully controlling pH and reactant stoichiometries has previously been reported by us (1) as well as by others (7). This ability to control the average pore diameter is a very desirable feature in catalyst preparation. In particular, Zou and Gonzalez (1) have shown that when the average pore diameter is matched to coincide with the particle size, metal sintering is minimized due to a decrease in the surface diffusion coefficient. This result was theoretically predicted by Ruckenstein and Pulvermacher (2, 3). Under conditions of low metal loading (<0.5 wt% Pt designed), it was found that $Pt/SiO_2$ xerogel catalysts resisted sintering at temperatures approaching 700°C. The hydrolysis of TEOS is first order in the concentration of $H_2O$ under acid conditions. For this reason, the concentration of hydrolized species is high and the rate-controlling step is the condensation reaction. Large BET surface areas and small average pore diameter were obtained for high $H_2O$/TEOS ratios. High $H_2O$/TEOS ratios increase the rate at which hydrolysis occurs. The BET surface area and pore volume of the materials obtained is highly dependent on the relative rates of hydrolysis and condensation.

*Effect of solvent removal.* Because of their superior thermal properties, aerogels have been used extensively as support materials. For this reason, a study on the effect of supercritical solvent extraction on the exposed metal surface area was undertaken. The data corresponding to this study is summarized in Table 4. The analysis of metal loading as measured by ICP shows that both the aerogels and the xerogels have similar metal contents (~0.80 wt% Pt). However, the metal dispersion obtained for the aerogels was discouraging. Results obtained using either $H_2$ or CO chemisorption were in agreement with results obtained using transmission electron microscopy. The BET surface areas and pore volumes for the aerogels were considerably larger than those obtained for the xerogels. This is due to the elimination of the interfacial menisci between liquid and vapor in the capillaries.

*Precursor adsorption onto the support.* A variety of procedures have been used to disperse metals onto aerogel (6). For example, Astier *et al.* (23) prepared $Pt/MoO_2$ by impregnating a $MoO_2$ aerogel with a solution of chloroplatinic acid in methanol. A ternary $CuZnO/Al_2O_3$ catalyst was prepared by impregnating an alumina aerogel with a copper and zinc acetate solution dissolved in methanol (24). In this study, a solution of $Pt(NH_3)_4(NO_3)_2$ suspended in warm acetone was impregnated onto a silica aerogel dissolved in ethanol. The resulting BET surface area was observed to increase slightly. However, the average pore diameter and pore volume decreased sharply (Table 7). Metal dispersions measured using both chemisorption and TEM were in agreement and results were poor in comparison to those obtained by synthesis in a homogeneous solution. Catalysts prepared by ion-exchanging $Pt(NH_3)_4(NO_3)_2$ onto the silica aerogel at a pH of 8.0 also resulted in low metal dispersions.

The collapse of the microstructure following impregnation is due to capillary forces at the ethanol interface during drying in an oven at 110°C. When the ion-exchange method was used, water and dilute $NH_4OH$ had to be added in order to adjust the pH to 8.0–9.0. Because surface tension for water and ethanol are 0.059 and 0.016 *N*/m, respectively, it is not surprising that further collapse of the microstructure occurred following drying at 100°C. Nicolaon and Teichner (25) pointed out that aerogels heated in air at 500°C retain almost no OR groups and become hydrophilic. For this reason, $Pt(NH_3)_4(NO_3)_2$ is adsorbed onto the surface of aerogels with difficulty and poor metal dispersions are obtained.

$Pt(AcAc)_2$ was also used to impregnate aerogel supports. It is important to note (Table 8) that when this metal precursor is used, microstructural collapse does not occur. This is due to the similarity between the organic metal precursor and the organic alkoxide on the support.

### $H_2$/*n*-Hexane Reactions

This reaction is typical of hydrocarbon reactions and can form products through hydrogenolysis, cyclization and isomerization. Because these reactions can be demanding, as in the case of cyclization or hydrogenolysis or fascile (isomerization), they offer an interesting base to compare the different catalysts prepared. The isomerization activity normally attributed to the acid function of the support has been eliminated in the present study as alumina has been replaced by silica. Observed selectivity and activity differences are due only to the metal function. Linear Arrhenius plots in the 260–330°C temperature range calculated on the basis of *n*-hexane conversion suggest that the reaction mechanisms do not change substantially over this temperature range. The activation energy for the overall reaction, 125 KJ/mole, was in good agreement with the value of 120 KJ/mole obtained by Martin *et al.* (26) over various Pt zeolites. All four catalysts had the same designed metal loading (1 wt% Pt) and comparable actual metal loadings between 0.65 and 0.91 wt% as measured by ICP. However, average particle sizes and particle size distributions were very different.

The $Pt/SiO_2$ xerogel and ion-exchange catalysts deactivate at a slower rate than the other $Pt/SiO_2$ catalysts tested. This deactivation as determined by the first order deactivation rate constant (Table 10) is dependent on particle size. This is, in part, due to the demanding nature of coke formation which is favored on large particles. However, a major advantage of high-surface-area materials is that metal interparticle distances are large and that coke can be accommodated more easily by this large surface area.

## CONCLUSIONS

The following conclusions emerge from this study:

(1) Variables which control the microstructure of silica prepared by the sol–gel method include: preparative pH,

reactant stoichiometries, and gelation temperature. High surface areas and well-defined pore diameters can be obtained using sol–gel processing. In particular, surface areas as high as 1000 m$^2$/g with microporous structure can be prepared at low pH (~1.3). At intermediate value of the pH (3–8), BET surface areas ranging from 850 to 350 m$^2$/g can be obtained. Pore structures are mesoporous with pore diameters ranging from 4 to 25 nm at a preparative H$_2$O/TEOS ratio of 10. Solvent extraction under supercritical conditions leads to high BET surface areas and large pore volumes.

(2) Because of repulsive interactions the use of $H_2PtCl_6 \cdot xH_2O$ as the metal precursor results in poor Pt dispersions. When $Pt(NH_3)_4(NO_3)_2$ is used, the precursor–support interactions become attractive and high dispersions are obtained. However, BET surface areas and pore volume are difficult to control. The use of Pt(AcAc)$_2$ was found to be the most flexible metal precursor. Solubility in acetone is high, and surface areas and pore volumes are more easily controlled.

(3) Unlike catalysts prepared by the ion-exchange method, the designed metal loading is an important variable in dispersing metals on supports prepared by the sol–gel method. Average pore diameters in the 4–20 nm range can be obtained by adjusting the H$_2$O/TEOS ratio during synthesis. In order to insure complete conversion of the TEOS, H$_2$O/TEOS ratios in excess of 10 should be used.

(4) Xerogels were superior to aerogels in promoting high metal dispersions. $Pt(NH_3)_4(NO_3)_2$ or Pt(AcAc)$_2$ are both difficult to impregnate onto silica aerogels. Ion-exchange methods are not recommended to disperse metals on aerogels.

(5) Pt/SiO$_2$ xerogel catalysts prepared by the sol–gel method are at least as active as catalysts prepared by ion exchange. In addition to this high catalytic activity, they are resistant to catalyst deactivation by the formation of coke and are considerably more resistant to sintering than catalysts prepared by ion exchange.

(6) When the H$_2$/*n*-hexane reaction is carried out at 400°C, there is a small decrease (~10%) in metal dispersion, BET surface area and pore volume. The loss can be partially restored through oxidation at 425°C for relatively long periods of time (16 h).

## ACKNOWLEDGMENTS

The authors acknowledge support from the Petroleum Research Fund of the American Chemical Society (ACS-PRF 26247-AC5) for this research. Partial support from the U.S. Department of Energy (Grant DOEFG02-86ER-1351) is also gratefully acknowledged. We also acknowledge the Electron Microscopy Laboratory at Tulane University for the use of their facility. We also acknowledge Professor J. B. Butt for supplying samples in this comparative study.

## REFERENCES

1. Zou, W., and Gonzalez, R. D., *Appl. Catal. A: General* **102,** 181 (1993).
2. Ruckenstein, E., and Pulvermacher, B., *J. Catal.* **29,** 224 (1973).
3. Ruckenstein, E., and Pulvermacher, B., *J. Catal.* **37,** 416 (1975).
4. Fricke, J., (Ed.), *"Aerogels,"* Springer-Verlag, Berlin/New York, 1986.
5. Brinker, C. J., and Scherer, G. W., "Sol–Gel Science", Academic Press, San Diego, 1990.
6. Pajonk, G. M., *Appl. Catal.* **72,** 217 (1991).
7. Teichner, S. J., Nicolaon, G. A., Vicarini, M. A., and Gardes, G. E. E., *Adv. Colloid Interface Sci.* **5,** 245 (1976).
8. Blanchard, F., Pommier, B., Reymond, J. P., and Teichner, S. J., *J. Mol. Catal.* **17,** 171 (1982).
9. Zou, W., and Gonzalez, R. D., *J. Catal.* **133,** 202, (1992).
10. Gonzalez, R. D., and Sarkany, J., *J. Catal.* **76,** 75 (1982).
11. Sing, K. S. W., Everett, D. H., Haul, R. A. W., Moscou, L., Pierroti, R. A., Roquerol, J., and Siemieniewska, T., *Pure Appl. Chem.* **57,** 603 (1985).
12. Zou, W., and Gonzalez, R. D., *Catal. Today,* **15,** 443 (1992).
13. Brunelle, J. P., *Pure Appl. Chem.* **50,** 1211 (1978).
14. Uchijima, T., Herrmann, J., Inoue, Y., Burwell, R. L., Butt, J. B., and Cohen, J. B., *J. Catal.* **50,** 464 (1977).
15. Levenspiel, O., "Chemical Reaction Engineering," pp. 537–551. Wiley, New York, 1972.
16. Keefer, K. D., in "Better Ceramics through Chemistry" (C. J. Brinker, D. J. Clark, and D. R. Ulrich, Eds.), pp. 15–24. North-Holland, New York, 1984.
17. Aelion, R., Loebel, A., and Eirich, F., *J. Am. Chem. Soc.* **72,** 5705 (1950).
18. Iler, R. K., "The Chemistry of Silica," Wiley, New York, 1970.
19. Lopez, T., Romero, A., and Gomez, R., *J. Non-Cryst. Solids* **127,** 105 (1991).
20. Armor, J. N., Carlson, E. J., and Zambri, P. M., *Appl. Catal.* **19,** 339 (1985).
21. Lopez, T., Herrera, L., Gomez, R., Zou, W., Robinson, K., Gonzalez, R. D., *J. Catal.* **136,** 621 (1992).
22. Zou, W., and Gonzalez, R. D., submitted for publication.
23. Astier, M., Bertrand, A., and Teichner, S. J., *Bull. Soc. Chim. Fr.* 191 (1980).
24. Pommier, B., and Teichner, S. J., "Proceedings, 9th International Congress on Catalysis, Calgary, 1988" (M. J. Phillips and M. Ternan, Eds.), Chem. Institute of Canada, Vol. 2, p. 610. Ottawa, 1988.
25. Nicolaon, G. A., and Teichner, S. J., *Bull. Soc. Chim. Fr.* 4343 (1968).
26. Martin, A. M., Chen, J., John, V. T., and Dadyburjor, D. B., *Ind. Eng. Chem. Res.* **28,** (11), 1613 (1989).